Anisotropic magnetism in $NdCrSb_3$

2008 J. Phys.: Condens. Matter 20 295226

(http://iopscience.iop.org/0953-8984/20/29/295226)

J. Phys.: Condens. Matter **20** (2008) 295226 (4pp) doi:10.1088/0953-8984/20/29/295226

Anisotropic magnetism in $NdCrSb_3$

Manjusha Inamdar, A Thamizhavel and S Ramakrishnan

Tata Institute of Fundamental Research, Mumbai-400005, India

E-mail: ramky@tifr.res.in

Received 20 April 2008, in final form 16 June 2008
Published 1 July 2008
Online at stacks.iop.org/JPhysCM/20/295226

Abstract

We report anisotropic dc magnetic susceptibility $\chi(T)$, isothermal magnetization $M(H)$, electrical resistivity $\rho(T)$ and heat capacity $C(T)$ measurements on a high quality single crystalline sample of $NdCrSb_3$. The crystal exhibits ferromagnetic ordering below $T_C = 100$ K due to ordering of Cr spins. The ferromagnetic phase is highly anisotropic. The anisotropy becomes even more evident at low temperatures where the rare earth ion (Nd^{3+}) gets magnetically ordered. Nd moments order ferromagnetically below 10 K. The magnetic interplay between these two species (Cr^{3+} and Nd^{3+} ions) gives $NdCrSb_3$ a complex magnetic phase diagram.

1. Introduction

Recent investigations [1–5] revealed that $RCrSb_3$ forms an interesting magnetic system which crystallizes in an orthorhombic structure, space group $Pbcm$. The quasi-2D crystal structure consists of infinite RSb and $CrSb_2$ layers stacked along the a axis. This layered system displays a variety of magnetic phenomena due to interplay between Cr 3d electrons and rare earth 4f electrons. Many members of this series have been well studied. $LaCrSb_3$, the first member of the series has a rich magnetic phase diagram [6]. It has been conjectured that both itinerant and local moments of Cr are involved in ferro and antiferromagnetic ordering respectively in the same compound [7]. $LaCrSb_3$ undergoes a ferromagnetic ordering at 125 K due to ordering of the itinerant moments of Cr^{3+} ions. Also along the c axis the local moments of Cr order antiferromagnetically (AFM) at 96 K. This antiferromagnetic transition gets suppressed with the application of moderate magnetic fields. Recent studies [8–11] show other members such as $CeCrSb_3$, $SmCrSb_3$ and $GdCrSb_3$ display an interesting interplay of Cr and rare earth moments. Earlier a brief account of the magnetization, magnetoresistance and neutron diffraction studies on single crystal and a powder of crystallites of $NdCrSb_3$ have been reported by Deakin *et al* [12]. Their investigations demonstrated the occurrence of ferromagnetism of Cr spins at 107.8 K with the easy axis of magnetization along the b axis. These spins couple ferromagnetically with Nd spins that order ferromagnetically below 12.7 K with a change of the easy axis of magnetization from the b to a axis. However, they have reported measurements of the magnetization of a powder sample and resistivity only along the c axis. In this work we provide a comprehensive study of the bulk properties of a high quality single crystal of $NdCrSb_3$ which exhibits a rich magnetic phase diagram with a large anisotropy due to the interaction of Cr^{3+} and Nd^{3+} moments.

2. Experimental details

The single crystals of $NdCrSb_3$ were grown by the self flux method. The starting materials of 3N pure rare earth and Cr, and 5N pure Sb were taken in an off-stoichiometric composition with Nd, Cr and Sb metals in the ratio 1:2:20. The metals were placed in a high quality recrystallized alumina crucible and subsequently sealed in a quartz ampoule. The quartz ampoule was heated to 1050 °C and held there for two days in order to achieve proper homogenization of the melt. After homogenization, the ampoule was slowly cooled down to 650 °C, just above the melting point of Sb, then brought down to room temperature at a faster rate. The single crystals present in the solidified Sb flux matrix were removed by means of a centrifuge. The phase of the sample was confirmed by performing powder x-ray diffraction on few ground single crystals. The Rietveld refinement of the x-ray pattern resulted in orthorhombic lattice constants $a = 12.955(5)$ Å, $b = 6.164(4)$ Å and $c = 6.052(3)$ Å with reliability parameters $R_B = 10\%$ and R_F factor $= 6.05\%$. From Laue back scattering pictures the largest surface was found to be perpendicular to a axis. The crystal structure is shown in figure 1. The high quality of the crystal was ascertained by sharp Laue reflection and EDAX analysis. The structure (space group $Pbcm$) shown in figure 1 consists of anionic layers parallel to the (100) plane separated by Nd^{3+} cations. One layer contains octahedra where Cr is coordinated

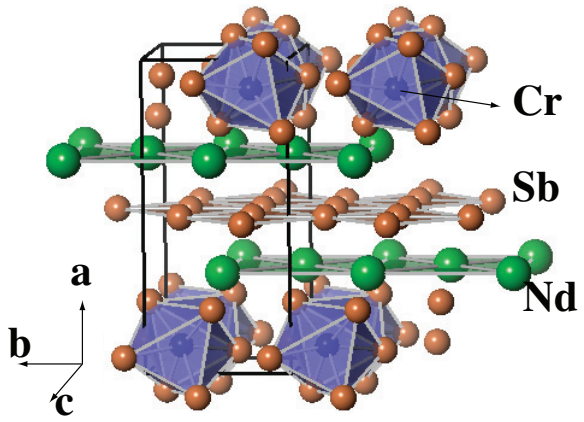

Figure 1. The crystal structure of $NdCrSb_3$ consists of four formula units with 20 atoms in the unit cell. The unit cell has a single site for Nd atom with position symmetry 0.308, 0.0024 and 0.25; three types of Sb atoms with position symmetry 0.0628, 0.1064, 0.2500; 0.2159, 0.4989, 0.2500; 0.5011, 0.2500, 0.0000 and one type Cr atom with the position symmetry 0.9095, 0.2500, 0.0000.

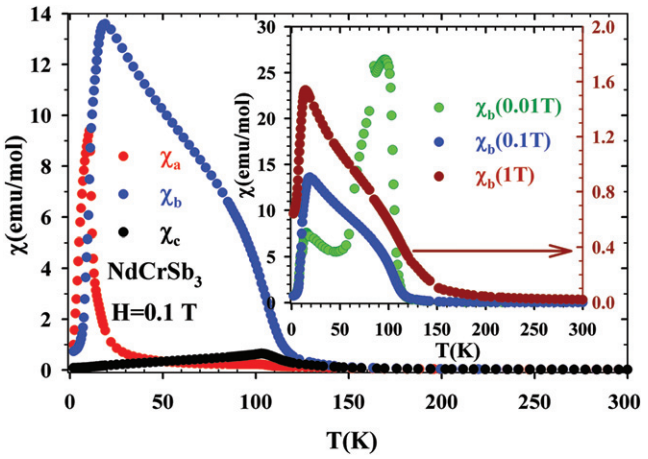

Figure 2. Panel (a) shows the susceptibility ($\chi(T)$) for all the axes for $NdCrSb_3$ down to 2 K from room temperature at 0.1 T of field. The inset shows the temperature dependence of the susceptibility along the b axis at 0.01, 0.1 and 1 T. Note that in a field of 1 T, the value of the susceptibility is small and it is represented by the $Y1$-axis (right).

by six Sb(1) and Sb(2) atoms that are face-sharing along the c-axis and edge-sharing along the b-axis, while the other layer is a nearly square sheet of Sb(3) atoms. The Nd atoms are nine-coordinated, forming a monocapped antiprism whose capping Sb(1) atom is tilted to one side. This structure can be visualized as an effective 2D structure with infinite layers of NdSb and $CrSb_2$ perpendicular to a-axis. This provides the basis for the observed anisotropy in the bulk properties of $NdCrSb_3$ and Cr ions seem to be in the trivalent state from the bond length considerations while the rare earth ions adopt the natural trivalent state except Yb which is claimed to be in the divalent state in $YbCrSb_3$ [2]. The temperature dependence of the magnetic susceptibility $\chi(T)$ along the individual axis (a, b and c) was measured using a commercial SQUID magnetometer (MPMS5, Quantum Design, USA). The resistivity $\rho(T)$ between 1.5 and 300 K was measured using an LR700 resistance bridge (Linear Research, USA) by the 4-probe method with contacts made using silver paste. The in-field and zero field heat capacity $C(T)$ between 5 and 200 K was measured using the commercial PPMS (Quantum Design, USA).

3. Results and discussion

We will first discuss here results from our iso-field and isothermal magnetization measurements along the three axes. Figure 2 shows the temperature dependence of anisotropic dc susceptibility ($\chi(T)$) data along the a, b, and c axes in an applied field of 0.1 T. The susceptibility (χ) along all axes show a sharp anomaly at $T_C = 100$ K. This anomaly is attributed to ferromagnetic ordering of Cr moments which is also observed in other members of this family ($RCrSb_3$). The anisotropy in the magnetic properties of this system is evident as we see the value of χ is much higher along the b axis as compared to that of the other two axes. The ratio χ_b/χ_a is almost 1.6 and χ_b/χ_c is 40 at 10 K, giving the measure of anisotropy in the system. The values of χ suggest that b is an easy axis for Cr moments ordering. Below T_C the magnetic phase diagram seems complicated. The magnetization falls immediately after T_C along the a and c axes. The smallness of the magnetization along the c axis confirms it to be the hard axis of the magnetization. To illustrate the field dependence on the susceptibility, we show the temperature dependence of the χ data along the b axis at 0.01, 0.1 and 1 T in the inset of figure 2. At even lower temperatures the magnetization starts to increase until we see a sharp drop in $\chi(T)$ at $T_C = 10$ K, along all axes, which is attributed to ferromagnetic ordering of Nd moments. In addition at low fields (0.01 T), one can clearly distinguish the two ferromagnetic transitions due to Cr and Nd moments. At higher fields, the value χ reduces significantly due to the interaction between Nd and Cr moments. Similar behavior has also been observed in $PrCrSb_3$ [13] though Pr^{3+} moments order antiferromagnetically in that compound. An analogous temperature dependence at 0.01, 0.1 and 1 T is also observed along the a axis as shown by the figure 3. The high temperature magnetic susceptibility along all axes (not shown here) was fitted to a modified Curie–Weiss expression, $\chi = \chi_0 + C/(T - \theta)$. The value of χ_0 is 1×10^{-3} emu mol^{-1}. The Curie constant gives an effective moment of 5.2 μ_B as compared to 3.01 μ_B for $LaCrSb_3$. Assuming Cr^{3+} has a moment of 3.8 μ_B as in the case of $LaCrSb_3$ [6], we estimate 3.55 μ_B for Nd moment which is close to the free ion moment of Nd (3.6 μ_B for Nd^{3+}). The value of θ is positive as expected for ferromagnets and is about 115 K along all the axis. However, the large value χ_0 is also estimated from the high temperature susceptibility data (which is similar in magnitude to those estimated for other members of $RCrSb_3$) implying that the applicability of the Curie–Weiss relation to explain the temperature dependence of the $\chi(T)$ in this itinerant ferromagnetic system is not strictly valid. For further understanding of magnetic properties of $NdCrSb_3$ we have performed the isothermal magnetization measurements on the same crystal along all the three axes

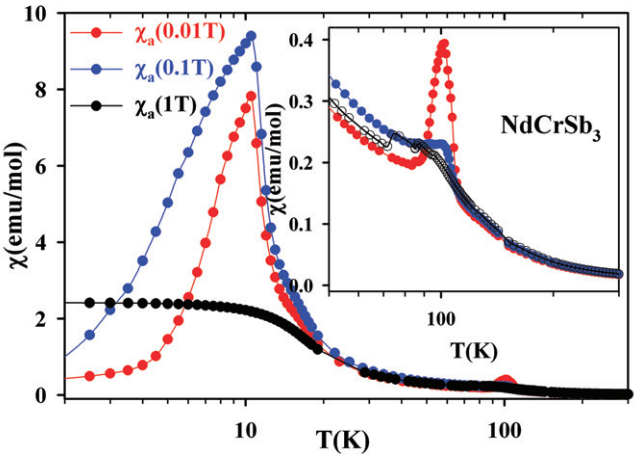

Figure 3. Temperature dependence of the susceptibility at 10 mT, 100 mT and 1 T along the a axis for $NdCrSb_3$. The inset shows the high temperature dependence of the susceptibility (χ_a) to illustrate the ferromagnetic transition of Cr moments at 100 K.

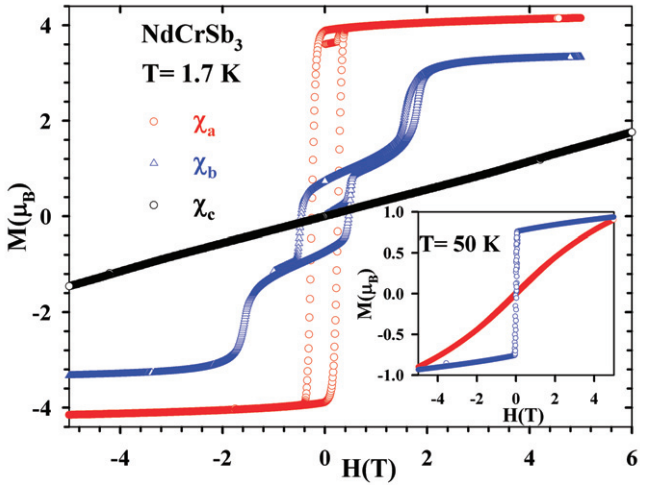

Figure 4. Magnetization versus field $\chi(H)$ (4-quadrant loop) for $NdCrSb_3$ along the a, b and c axes at 1.7 K. The inset shows the isothermal magnetization at 50 K. We see here the easy axis of magnetization re-orienting from b to a as we change the temperature from 50 to 1.7 K. The main panel also shows the ferromagnetic hysteresis along the a and b axes while the magnetization along the c axis does not exhibit any measurable hysteresis, suggesting that it is a hard axis of magnetization.

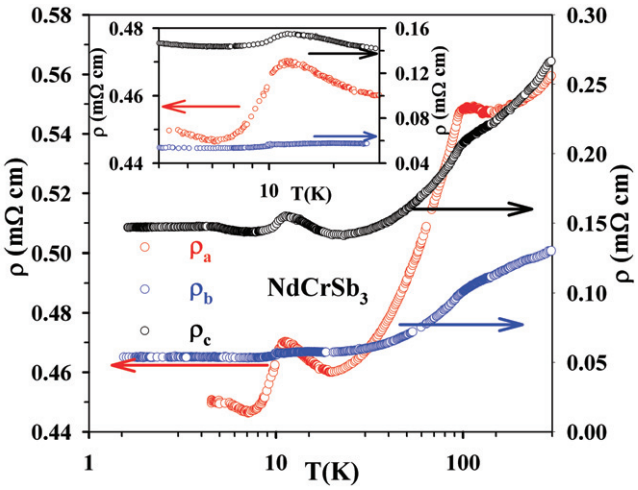

Figure 5. The main panel shows resistivity ρ versus temperature T data for the $NdCrSb_3$ system with current I along the a, b and c axes. The inset shows resistivity at low temperatures.

at temperatures 1.7, 10, and 50 K. For all the temperatures along the a and b axes the magnetization appears hysteretic. As seen in figure 4 the magnetization along the a and b axes tends to saturate to 4.2 and 3.7 μ_B respectively as compared to saturation moment of 1.5 μ_B for $LaCrSb_3$. The saturation moment has contributions both from Nd^{3+} and Cr^{3+} ions. The moments along the c axis do not saturate until 12 T. The high value of moments along a suggest that a is the easy axis for Nd moments. Clearly from our magnetic susceptibility and isothermal magnetization measurements we can say that $NdCrSb_3$ is ferromagnetic at all temperatures below T_C with the presence of ferromagnetism due to ordering of Nd moments giving the system a complicated magnetic phase diagram. This is further substantiated by the multiple transitions observed along the b axis as shown in figure 4. The ordering temperatures observed here are much lower compared to the polycrystalline report on this sample [5] where T_C = 141 K and T_{C1} = 13 K.

The resistivity $\rho(T)$ versus temperature data for the sample is shown in figure 5 for temperatures between 1.5 and 300 K for an excitation current I (5 mA) along individual axes. As expected the sample shows a sharp fall in $\rho(T)$ below T_C due to the decrease in the spin-disorder scattering at the ferromagnetic transition of the Cr moments. The sample exhibits anisotropy in its resistivity with room temperature values of $\rho_a(300\ \text{K}) = 560\ \mu\Omega$ cm, $\rho_b(300\ \text{K}) = 148\ \mu\Omega$ cm and $\rho_c(300\ \text{K}) = 268\ \mu\Omega$ cm for $NdCrSb_3$. Unlike the large anisotropy observed in the resistivity of $LaCrSb_3$ [6], the anisotropy ρ_a/ρ_c is only a factor of 2 at room temperature (RT), increasing to 3 at low temperatures ($T < 5$ K). However, the ratio ρ_a/ρ_b is 3.7 at RT which increases up to 10 below 5 K. The low temperature data show the anomaly at the ferromagnetic transition due to the ordering of Nd moments. It is important to note that our ρ data clearly shows anomalies at both ferromagnetic transitions (Cr as well as Nd ordering) in contrast to the absence of such anomalies in the published ρ data of Deakin *et al* [12]. This observation could be ascribed to the superior quality of our crystals. Another feature is the high temperature behavior of the resistivity along the a axis before T_C which shows an increase unlike the concave behavior shown by $\rho(T)$ along the b and c axes. This behavior observed in $LaCrSb_3$ [7] has been ascribed to FM ordering due to the super exchange mechanism, which is also responsible for the magnetic ordering observed in manganites.

The temperature dependence of the heat capacity $C_P(T)$ of $NdCrSb_3$ between 6 and 200 K is shown in the main panel of figure 6. Unlike $LaCrSb_3$ [7], we see a well defined anomaly in the heat capacity data of $NdCrSb_3$ at T_C = 100 K (shown in the inset (a)) though is considerably weaker than those observed in $CeCrSb_3$ [14] and $PrCrSb_3$ [13]. The anomaly at T_C gets smeared with the application of 1 T of field (not shown). The

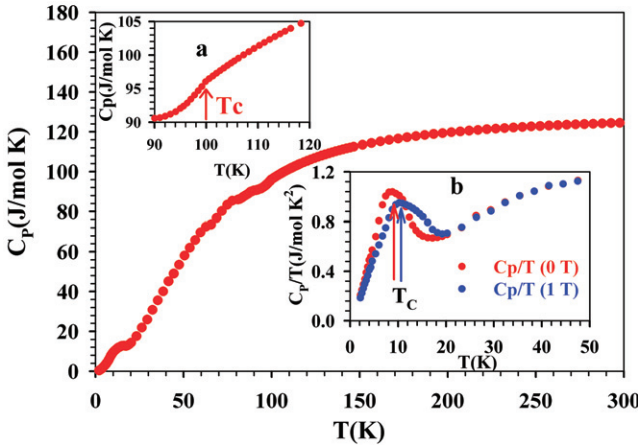

Figure 6. Specific heat versus temperature for the $NdCrSb_3$ sample. We see two well defined kinks in the data at the ferromagnetic transitions due to ordering of Cr moments (100 K) and Nd moments (10 K). The inset (a) shows the C_P data at high temperatures. The inset (b) shows the heat capacity data under 0 and 1 T with the anomaly due to ferromagnetic ordering of the Nd ions.

broadening of the heat capacity peak for $NdCrSb_3$ at T_C is supportive of the fact that Cr moments undergo a ferromagnetic transition. The inset (b) in the same figure shows the low temperature C_P data which establishes the bulk magnetic ordering of the Nd moments below 10 K. The broadening of the anomaly in a moderate field of 1 T confirms the bulk nature of the ferromagnetic ordering of the Nd moments.

4. Conclusion

To conclude, we have grown single crystals of the compound $NdCrSb_3$ by the flux growth method and characterized them by x-ray, Laue back scattering, dc magnetic susceptibility, isothermal magnetization, resistivity and heat capacity (0 and 1 T) measurements. All measurements confirm bulk ferromagnetic ordering of the Cr moments below 100 K in this compound. The presence of f moments of the Nd ion shifts the T_C to a lower value as compared to that of $LaCrSb_3$. The easy axis of magnetization for the Cr moments continues to be the *b* axis as in case of $LaCrSb_3$, $CeCrSb_3$ and $PrCrSb_3$. The Nd^{3+}–Cr^{3+} interaction gives a complex magnetic phase below T_C. This gives a different signature of $\chi(T)$ along all three axes. It is important to realize that although Cr orders ferromagnetically in all $RCrSb_3$ compounds, the nature of the magnetism exhibited by magnetic rare earth spins are different starting from the inhomogeneous ferromagnetism of Ce spins in $CeCrSb_3$ [11, 14], the antiferromagnetism of Pr spins in $PrCrSb_3$ [13] with a gap in the spin excitation spectrum and the ferromagnetic ordering of Nd spins in $NdCrSb_3$ (described in the present work and also in [12]). However, in $NdCrSb_3$ (unlike $CeCrSb_3$ [10, 14]) we see a sharp magnetic ordering due to the moments of Nd at 10 K. The easy axis for magnetization for the FM ordering is along the *a* axis and shifts to *b* at higher field. The resistivity and heat capacity measurements for $NdCrSb_3$ also show anomalies at these two ordering temperatures confirming our analysis of the magnetic properties of this system. Neutron scattering studies are underway for a detailed understanding of the magnetic phase of this compound.

References

[1] Brylak M and Jeitschko W 1995 *Z. Naturf.* B **50** 899
[2] Crerar S J, Deakin L and Mar A 2005 *Chem. Mater.* **17** 2780
[3] Ferguson M J, Hushagen R W and Mar A 1999 *J. Alloys Compounds* **249** 191
[4] Raju N P, Greedan J E, Ferguson M J and Mar A 1998 *Chem. Mater.* **10** 3630
[5] Leonard M, Saha S and Ali N 1999 *J. Appl. Phys.* **85** 4759
[6] Jackson D D, Torelli M and Fisk Z 2002 *Phys. Rev.* B **65** 014421
[7] Granado E, Martinho H, Sercheli M S, Pagliuso P G, Jackson D D, Torelli M, Lynn J W, Rettori C, Fisk Z and Osheroff S B 2002 *Phys. Rev. Lett.* **89** 107204
[8] Jackson D D and Fisk Z 2004 *J. Magn. Magn. Mater.* **256** 243
[9] Jackson D D and Fisk Z 2003 *J. Alloys Compounds* **377** 106
[10] Jackson D D and Fisk Z 2006 *Phys. Rev.* B **73** 024421
[11] Jackson D D, McCall S K, Karki A B and Young D P 2007 *Phys. Rev.* B **76** 064408
[12] Deakin L, Ferguson M J, Mar A, Greedan J E and Mills A S 2001 *Chem. Mater.* **13** 1407
[13] Inamdar M, Thamizhavel A and Ramakrishnan S 2008 *Phys. Rev.* B **77** 132410
[14] Inamdar M, Thamizhavel A and Ramakrishnan S 2008 *J. Magn. Magn. Mater.* at press